Talanta 112 (2013) 136–142

Contents lists available at SciVerse ScienceDirect

Talanta

journal homepage: www.elsevier.com/locate/talanta

A novel DPSO-SVM system for variable interval selection of endometrial tissue sections by near infrared spectroscopy

Guiyun Wang [a], Mingyu Ma [a], Zhuoyong Zhang [a,*], Yuhong Xiang [a], Peter de B. Harrington [b]

[a] Department of Chemistry, Capital Normal University, Beijing 100048, China
[b] Department of Chemistry and Biochemistry, Center for Intelligent Chemical Instrumentation, Clippinger Laboratories, Ohio University, Athens, OH 45701-2979, USA

ARTICLE INFO

Article history:
Received 5 January 2013
Received in revised form
5 March 2013
Accepted 7 March 2013
Available online 15 March 2013

Keywords:
Near infrared spectroscopy (NIR)
Discrete particle swarm optimization (DPSO)
Support vector machine (SVM)
Variable interval selection
Endometrial tissue
Cancer diagnosis

ABSTRACT

A novel method combining a discrete particle swarm optimization (DPSO) with a support vector machine (SVM) was proposed for the variable interval selection of tissue sections of endometrial carcinoma by near infrared spectroscopy. The DPSO-SVM algorithm includes a multi-stage screening. In each screening step, the DPSO was repeated 50 times using random sampling, and the frequencies that the variable intervals were selected among the 50 repeats were used to select the most probable intervals. The variable intervals with high probabilities were selected and further used in the next screening. Finally, the subset of variable intervals with the highest classification rate was considered as the optimal variable intervals. A synthetic data set mimicking the near infrared (NIR) spectra of tissue samples was applied to evaluate the performance of the DPSO-SVM. For the synthetic data, the classification rates were $74.9 \pm 0.9\%$ and 100% for the full spectral range and the six variable intervals selected by the DPSO-SVM. For the real endometrial tissue data, the entire spectral data gave an average accuracy of $69.5 \pm 0.5\%$, while the 20 variable intervals gave $98.5 \pm 0.3\%$. The results showed that the informative variables from the NIR spectra could be selected and high classification accuracy was achieved by the proposed approach.

1. Introduction

Endometrial carcinoma (EC) is one of the most common invasive gynecological cancers in women, with about 288,387 new cancer cases and 73,854 deaths annually worldwide [1]. Endometrial cancer incidence is rising in most Western countries, largely owing to increasing obesity of the population [2]. It is reported that the 5-year survival rate for endometrial cancer in its early stages is much higher than in the mid or terminal stage [3]. Consequently, early detection of endometrial cancer is urgently needed.

The current diagnostic methods for endometrial cancer mainly include cytological examination [4], fractional curettage [5], hysteroscopy [6], B-ultra examination [7], serum markers [8] and magnetic resonance imaging (MRI) [9]. However, these methods suffer from the need for an additional endometrial biopsy, long diagnostic time, and high cost. Moreover, the results of biopsy rely on a pathologist's expertise, which slows down the process and is prone to error. Near infrared spectroscopy (NIRS) [10] is a fast, convenient, inexpensive and non-destructive diagnostic method that can be coupled with chemometrics, yielding a fast and noninvasive method for early detection of endometrial cancer. NIRS has gained wide attention in various fields, such as pharmaceutical industry [11], environment [12], biodiesel [13], food [14] and biomedical sectors [15].

The near infrared spectrum (4000–13,000 cm^{-1}) arises from molecular overtones and combinations of C–H, N–H, and O–H bond vibrations. However, the spectrum also contains background variations that arise from scattering by particles, temperature variations, and instrumental noise. Variable or feature selection refers to the use of a subset of spectral measurements and in this instance selecting a discrete subset of NIR wavenumber measurements. By selecting the most informative variables, we can speed up the computations, decrease the influence of noise, and remove unwanted variations such as baseline drift, while adding numerical stability. Several papers have shown the benefits of feature selection with respect to using the entire spectrum [16–19].

The support vector machine (SVM) is useful in handling high-dimensional classification problems and has been recommended as an effective approach for classification [20–22]. However, there are regions of the NIR spectrum that are not as informative. Other regions may convey information that is either redundant or irrelevant and in some cases their inclusion could undermine the predictive power of the classification model. When the SVM is applied without considering variable selection, the dimension of

* Corresponding author. Tel.: +86 10 68902490; fax: +86 10 68903040.
E-mail addresses: gusto2008@vip.sina.com, zhangzhuoyong@139.com (Z. Zhang).

0039-9140/$ - see front matter © 2013 Elsevier B.V. All rights reserved.
http://dx.doi.org/10.1016/j.talanta.2013.03.016

the input space may be too high and could result in overfitting which would decrease the predictive ability of the classifier [23]. Consequently, variable selection is a crucial step to analyzing large datasets by reducing the dimensionality of the data, which improves SVM model efficiency and leads to better prediction accuracy [24,25].

The variable selection can be considered as an optimization process which maximizes the prediction performance of the model. Optimization algorithms, such as genetic algorithm (GA) [26], simulated annealing (SA) [27], and ant colony optimization (ACO) [28], have been applied to select the optimal subset of variables. A relatively new optimization technique, i.e., particle swarm optimization (PSO) has been used as an optimizer for many applications. Melgani et al. proposed a novel classification system based on particle swarm optimization (PSO) to improve the generalization performance of the SVM classifier on the basis of ECG data [29]. Ren and Zhou applied PSO-SVM to forecast traffic safety. Compared with the backpropagation neural network, the PSO-SVM performed better for traffic safety forecasting [30]. Cura presented a new PSO approach to the clustering problem. Researchers tested the algorithm on two artificial and five real data sets and reported that the algorithm was an effective classifier [31]. However, particle swarm optimization applied to the field of spectroscopy as a variable interval selection method of endometrial tissue sections has not yet been reported.

In the present work, the combination of discrete PSO and SVM was proposed for the classification of endometrial cancer tissue samples. The discrete PSO algorithm was applied to select informative intervals and the SVM was used to build the classification model. By applying to an authentic and a simulated NIR spectral dataset, the DPSO-SVM proved to be a promising procedure for interval selection to achieve better prediction accuracy.

2. Theory and algorithm

2.1. Particle swarm optimization

Particle swarm optimization (PSO), which models the social behavior of groups of animals, is one of the modern heuristic algorithms for optimization. The algorithm, originally proposed by Kennedy and Eberhart in 1995 [32], is designed to avoid local minima by having a group of search directions that follow the optimal direction. Compared to other optimization algorithms, PSO is easy to implement, computationally efficient, converges faster, and has fewer parameters to be adjusted [33]. For PSO, each solution is a particle in the search space. To determine the optimal solution, each particle adjusts its searching direction according to its own experience and all the other particles' experiences.

The standard PSO algorithm is briefly introduced as follows. The PSO is initialized with a group of random particles in D-dimensional search space. The position of the ith particle at the nth iteration is represented as $x_i^n=(x_{i1}^n,x_{i2}^n,\ \ldots,x_{id}^n)$, for which x is the preparative optimization value. The velocity is described as $v_i^n=(v_{i1}^n,v_{i2}^n,\ \ldots,v_{id}^n)$. The optimal position of the ith particle at the nth iteration is $p_i^n=(p_{i1}^n,p_{i2}^n,\ \ldots,p_{id}^n)$, and $p_g^n=(p_{g1}^n,p_{g2}^n,\ \ldots,p_{gd}^n)$ is the optimal position of all the particles at the nth iteration. In iteration, each particle changes its own position and velocity according to the following equations:

$$v_{id}^n=wv_{id}^{n-1}+c_1r_1(p_{id}^n-x_{id}^n)+c_2r_2(p_{gd}^n-x_{id}^n) \tag{1}$$

$$x_{id}^{n+1}=x_{id}^n+v_{id}^n \tag{2}$$

for which d is the dimension, w represents the inertia weight factor, c_1 indicates the cognition learning factor, c_2 indicates the social learning factor, and r_1 and r_2 are random numbers in the range [0, 1]. By a large number of experiments, Carlisle and Dozier [34] proposed parameter settings, c_1 of 2.8 and c_2 of 1.3, which were used in this study.

2.2. Discrete particle swarm optimization

The PSO algorithm was designed to optimize continuous parameters, but many actual problems are discrete or combinatorial optimization problems. To solve the problem, Kennedy and Eberhart developed a discrete binary version of the particle swarm algorithm [35]. In the discrete PSO, a particle is composed of a binary variable, which moves in a space restricted to 0 and 1 in each dimension; and then the previous particle-position-update formula becomes inapplicable. The solution to this problem is that the velocity is defined as the probability of position taking the value 1. Afterwards, a logistic sigmoid function is used to transform the velocity in the interval [0.0, 1.0]. The new particle position is defined by the following rule:

$$x_{id}^{n+1}=\begin{cases}1, & \text{if } rand\le sig(v_{id}^{n+1})\\ 0, & \text{else}\end{cases} \tag{3}$$

for which

$$sig(x)=\frac{1}{1+e^{-x}} \tag{4}$$

The output of the DPSO feature selection algorithm is a binary vector composed of ones that correspond to the selected features and zeros that correspond to the rejected features.

2.3. Support vector machines

A support vector machine (SVM) is used here to build classifiers for normal, hyperplasia, and malignant tissue sections. SVM, a learning machine based on statistical learning theory, was first proposed by Vapnik in 1995 [36]. A SVM based on the Vapnik–Chervonenkis (VC) theory and the structural risk minimization (SRM) principle balances minimizing the generalization error and maximizing the geometric margin, to achieve the best generalization ability. For linearly separable data, SVM determines the optimal hyperplane, one that maximizes the separating margin and functions as the separating plane for the classification of input data. For linearly non-separable data, a kernel function can be found to map the input data into a higher dimensional feature space that is linearly separable. In this study, a linear kernel function is used and assumes that the NIR data are linearly separable.

2.4. Variable interval selection based on DPSO-SVM

This study developed a new DPSO-SVM approach for the variable interval selection of the NIR spectra of endometrial carcinoma tissue sections. The DPSO algorithm was applied to select intervals and the SVM was used as the classifier. The proposed variable interval selection procedure based on the DPSO-SVM is as follows:

(1) The full spectrum is split into equidistant sub-intervals.
(2) Randomly generate initial particles. Each particle is encoded to a string of binary bits (0 and 1) corresponding to spectral intervals, for which 1 represents a selected interval, and 0 indicates that the interval is discarded.
(3) Calculate the fitness function of the each particle. The fitness is defined as the negative of classification accuracy of SVM for the prediction set. Set the best position of each particle with its initial position. Find the best global position in the swarm with the minimal value of fitness.

(4) Update the velocity and the position of each particle according to Eqs. (1) and (3), respectively.
(5) Calculate the fitness of the renewed population. Update the best position of each particle if its current position has a smaller fitness.
(6) If the maximum number of iterations has not yet reached the pre-determined value, return to Step 2. Otherwise, output the best particles.
(7) The above algorithm is repeated for N times ($N=50$ in this study). The average of the N solutions is the best solution. Then, every spectral interval is exhibited in the form of probability. The intervals, for which the probability reaches a specific threshold, are retained to the next stage of iteration.
(8) Stop the procedure if the termination criterion is satisfied. Otherwise, return to Step 2. Spectral intervals without contribution or with a small contribution to the prediction ability of the model are eliminated during each screening cycle.
(9) Build the SVM model using the final selected variable intervals. The final variable intervals gave the best classification accuracy of the prediction set. A flowchart summarizing the DPSO-SVM is presented in Fig. 1.

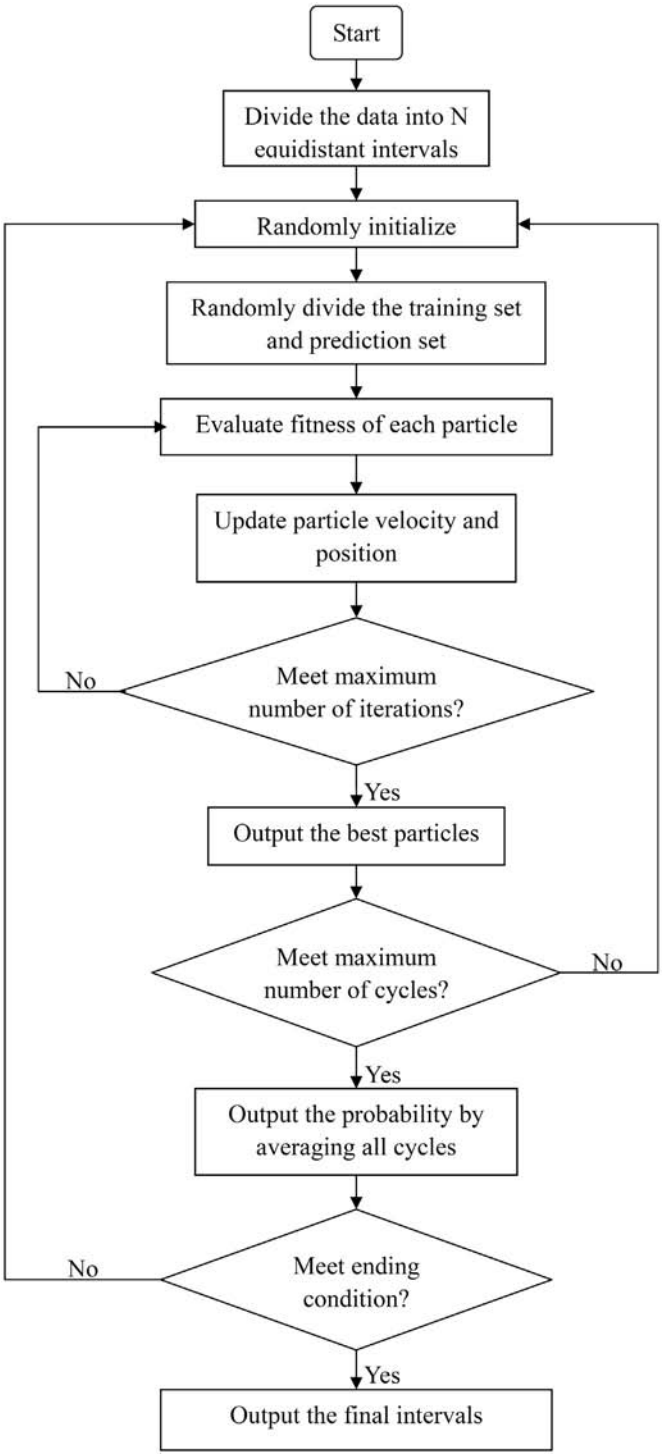

Fig. 1. Flowchart of the proposed DPSO-SVM for variable interval selection.

3. Experimental section

3.1. Apparatus

A Nicolet 6700 extended Fourier transform near infrared (FT-NIR) spectrometer equipped with an InGaAs detector (Thermo Electron, USA) was used for the NIR measurements. The spectrometer was controlled by the Thermo Fisher Omnic software, version 7.3. All programs were implemented in the MATLAB environment (The MathWorks Inc., South Natick, MA, USA).

3.2. Samples

Seventy-seven paraffin sections of endometrial tissues sections (18 normal, 30 hyperplastic, and 29 cancerous) were supplied by Beijing Obstetrics and Gynecology Hospital, attached to the Capital Medical University. The average age of the patients was 46 years, with a maximum of 71 and minimum of 19. All the endometrial tissues were stabilized in a 4% formaldehyde solution as received, and rinsed with a gradient concentration of ethanol solutions upon use. The samples were put into xylene, embedded in paraffin wax, and then sliced into 4 μm-thick sections. Each section was placed on a glass slide and dried at 45 °C. The area of each tissue sample slice on the glass slide was about 2 cm^2. Finally, they were fixed with a neural gum mounting.

3.3. NIR spectra measurements

The NIR diffuse reflection spectra were recorded with the integrating sphere of the FI-NIR spectrometer. Each spectrum had a nominal optical resolution of 4 cm^{-1} and was obtained from the average of 64 scans spanning the spectral range from 4000 to 10,000 cm^{-1}. The interval between spectral data points was 2 cm^{-1}. Each sample section was scanned at five different positions, and the average spectrum was used for each data object. The NIR spectrometer is sensitive to environmental conditions such as temperature and humidity. Therefore, the background spectrum was acquired using an air reference at 25 °C every 30 min.

3.4. Synthetic data

The synthetic data set comprised 100 objects and 3000 variables. Noise in the form of normally distributed random deviates with a mean of zero and standard deviation of 0. 1 was added to each data point. Eighty simulated Gaussian peaks at random positions, with amplitudes of 1 and standard deviations of 100, were added to half of the objects as backgrounds. Because the objects containing simulated backgrounds were selected randomly, the backgrounds are independent from the signal. A single Gaussian peak at a location of 1500 of the 3000 points with amplitude of 0.5 and a standard deviation of 50 was randomly added to 50% of the objects and these objects were assigned as class A. The other objects with the null signal were assigned as class B.

3.5. Data analysis

A bootstrapped Latin partition re-sampling method was used to evaluate SVM classification model. The data set is randomly partitioned into four parts with identical class distributions [37]. Three parts are used for model building and the other part is used for prediction. Each spectrum is predicted once and only once among the Latin partitions across each bootstrap so the results can be pooled to yield predictions for the entire data set. The results from the four prediction sets were pooled for each bootstrap. The classification accuracies were averaged across the 100 bootstraps and accompanied by their 95% confidence intervals.

4. Results and discussion

4.1. Synthetic data evaluations

The SVM classifier was applied to the full synthetic data set. The average accuracy using the entire spectral range for the four Latin partitions and 100 bootstraps was $74.9 \pm 0.9\%$. The SVM was operated with a linear kernel and the mediocre classification rate indicates that the classes are not linearly separable. Therefore, the DPSO algorithm was used to select the variables contributing the most to the SVM modeling. In the present work, the population size of the PSO was set as 200 and the maximum number of iterations was 300. The spectra of the synthetic data set were divided into 300 equidistant intervals (width of each interval is about 10 points). The mean prediction accuracies and the 95% confidence intervals were calculated from the results of the 100×4 bootstrapped Latin partitions.

Fig. 2 demonstrates the variation of the average accuracies of the prediction set for every screening of the synthetic data. In Fig. 2, first the average prediction rates increased quickly and the 95% confidence intervals decreased, which were due to the elimination of uninformative variables, then not much change due to the loss of redundant variables, and finally the performance decreases because of the loss of informative variables. The optimal variable intervals with probabilities greater than 0.85 were selected. The highest classification rate achieved was 100% while reducing the number of spectral elements from 3000 to 60. Fig. 3 gives the selected intervals for synthetic data. The red line displays the pure signal components in Fig. 3. These selected intervals located at 1341–1350, 1441–1450, 1491–1510, 1551–1560 and 1621–1630 point numbers are consistent with the signal.

To validate the proposed method, another data set of synthetic data using the same parameters was generated. The average prediction rate using the full data point and selected 60 data point was $75.2 \pm 0.9\%$ and $99.8 \pm 0.1\%$ respectively. The above results prove that DPSO-SVM is a promising method for variable interval selection. The DPSO-SVM significantly reduced the number of variables and achieved improved classification accuracy.

4.2. Cancerous tissue data evaluations

Based on our previous research, the spectra were converted to their second derivatives using the Savitzky–Golay algorithm by means of a nine-point cubic polynomial followed by multiplicative scatter correction (MSC) [38]. MSC pretreatment was used to correct the scattered light effects, which were caused by particles in tissue sample and the thickness of sections. The second derivative transform improves the resolution of peaks and reduces the baseline drift caused by scattering. Fig. 4 gives the spectra after the MSC and second derivative using the Savitzky–Golay algorithm.

The average accuracy of the full spectra was $69.5 \pm 0.5\%$. So, it was decided to see if feature selection would improve the classification rate. The parameters of PSO were the same in both cancerous tissue data and the synthetic data. The NIR spectra of endometrial carcinoma were divided into 311 equidistant intervals (wavelength of each interval is about 17 cm^{-1}).

Fig. 5 demonstrates that the mean prediction accuracies with selected variables in each screening with 95% confidence intervals. As illustrated in Fig. 5, at the beginning, the mean value was small and the 95% confidence interval was comparatively large. With the increase of probability, however, the prediction accuracy increased gradually and reached the highest accuracy ($98.5 \pm 0.3\%$) when the probability was 0.65. The prediction accuracy reached the maximum when the probability was 0.65, whereas using more or less variables

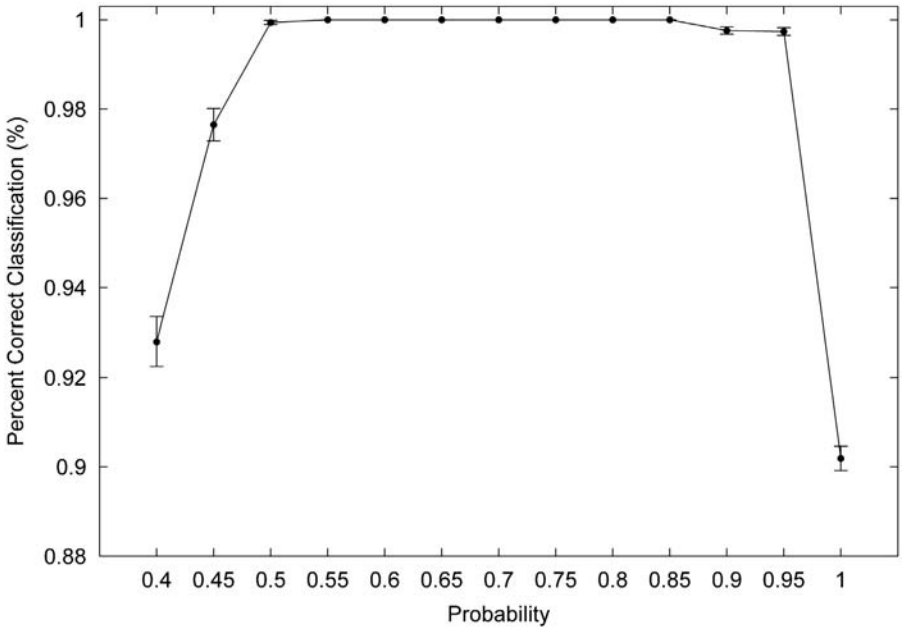

Fig. 2. Average prediction accuracies and 95% confidence intervals with selected variables each screening for synthetic data.

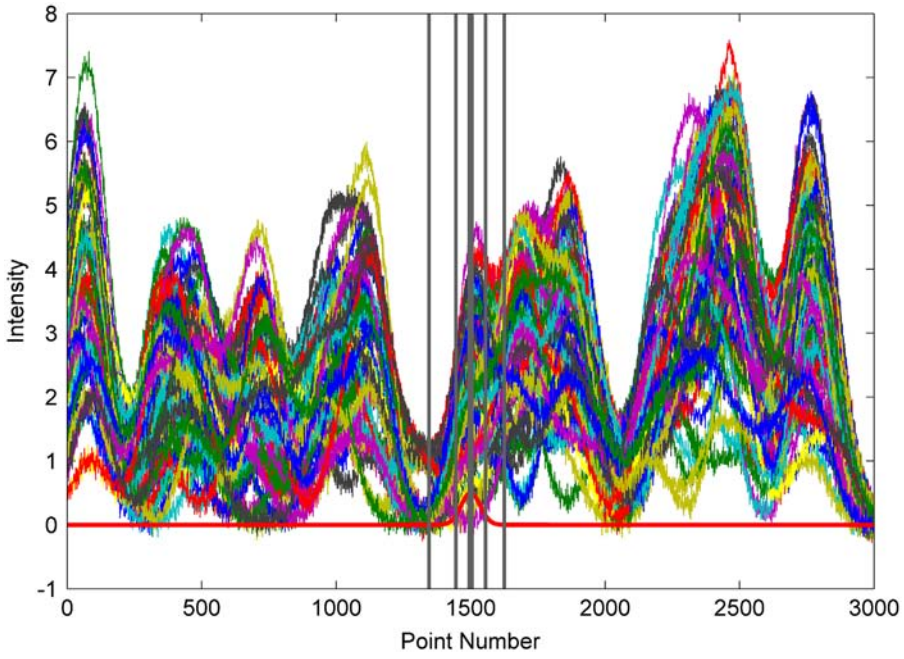

Fig. 3. Selected spectral intervals for synthetic data with pure signal component in red. (For interpretation of the references to color in this figure legend, the reader is referred to the web version of this article.)

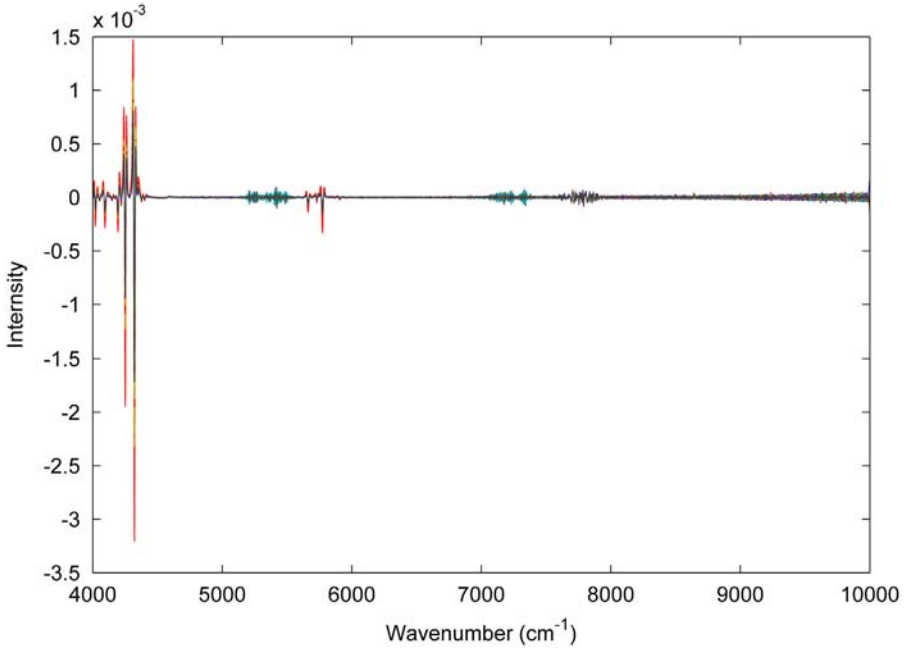

Fig. 4. NIR reflectance spectra after MSC and second derivative using the Savitzky–Golay.

would decrease the accuracy. The best model had maximum classification accuracy with 20 selected intervals (200 variables).

Selected spectral intervals are provided in Fig. 6. The absorption band from 4272 to 4289 cm^{-1} can be ascribed to the first combinations of the C–H vibrations of the molecules. The absorption band from 6219 to 6237 cm^{-1} can be assigned to the first overtones of the C–H vibrations. The absorption bands from 6933 to 6950 cm^{-1} and from 7589 to 7606 cm^{-1} can be assigned to the second combinations of the C–H vibrations. The absorption bands in the ranges of [7936, 7953] cm^{-1}, [8283, 8300] cm^{-1}, [8514, 8532] cm^{-1}, [8649, 8667] cm^{-1}, [8746, 8763] cm^{-1}, [8842, 8860] cm^{-1}, and [8996, 9014] cm^{-1} can be assigned to the second overtones of the C–H vibrations. The absorption bands in the ranges of [9266, 9284] cm^{-1}, [9575, 9592] cm^{-1}, [9614, 9631] cm^{-1}, [9671, 9689] cm^{-1}, [9787, 9805] cm^{-1}, and [9864, 9882] cm^{-1} correspond to the third combinations of the C–H bond. Such results are reasonable because the main differences in tissue composition between normal, hyperplasia and cancer tissues are from DNA, water content, lipids and proteins. These tissue composition differences will contribute to the spectral variance between cancer, hyperplasia and normal tissue samples. The above results suggest that good prediction accuracy can be obtained using the selected spectral intervals, which demonstrate the importance and effectiveness of variable interval selection.

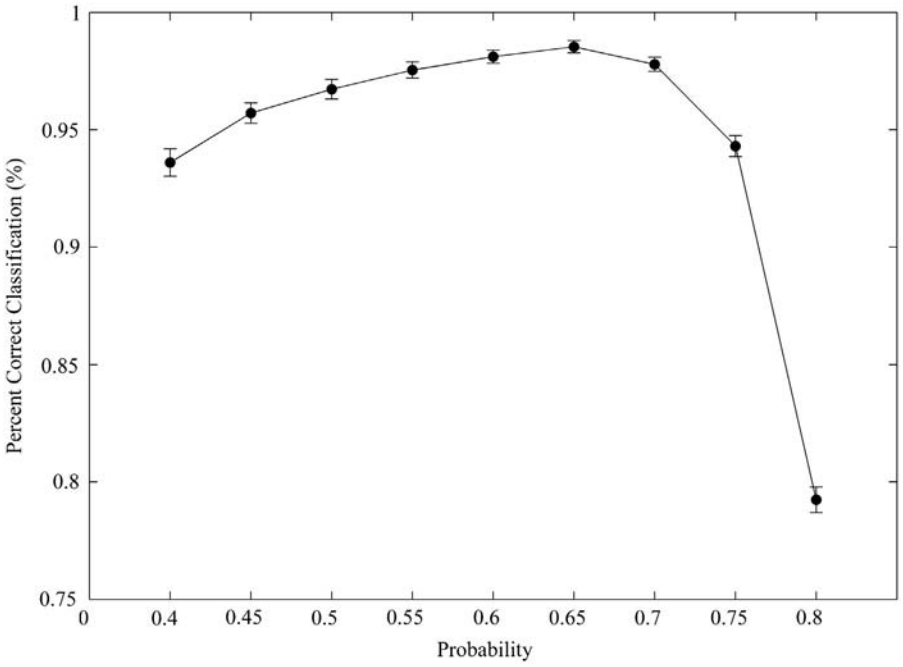

Fig. 5. Mean prediction accuracies and the 95% confidence intervals with selected variables each screening for cancerous tissue data.

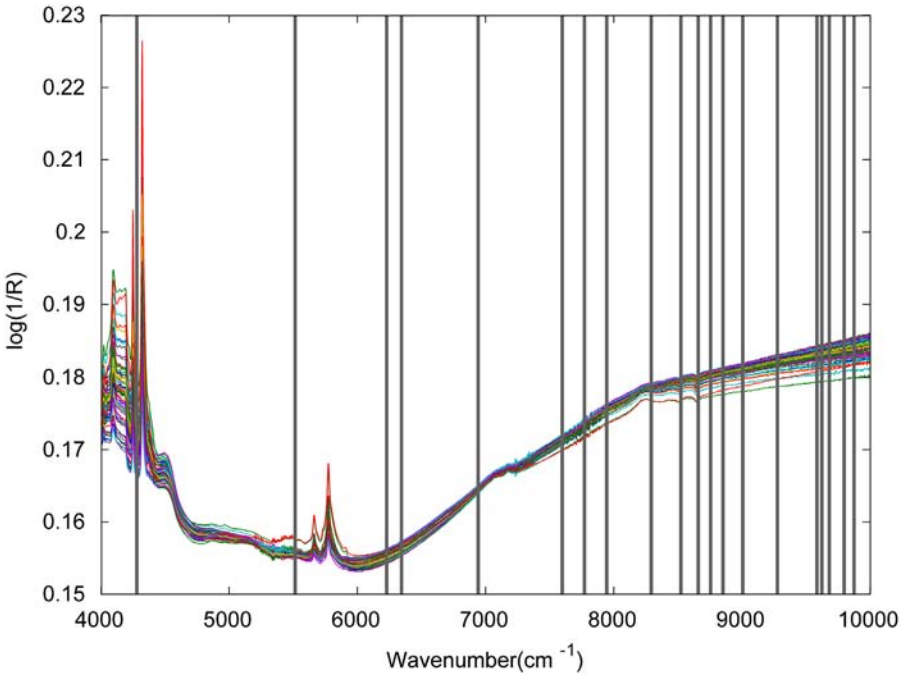

Fig. 6. Selected spectral intervals for cancerous tissue data after MSC.

5. Conclusions

NIR spectra of tissues contain redundant or uninformative variables that may deteriorate the predictive performance of the classification model. In this paper, discrete particle swarm optimization (DPSO) combined with support vector machine (SVM) was proposed for the selection of informative variables. The synthetic data set and the cancerous tissue data set were used by the proposed DPSO-SVM algorithm. Experimental results demonstrated that the proposed DPSO-SVM approach effectively selected features to build an optimal classifier with high accuracy. Therefore, DPSO-SVM has promise for the early diagnosis of endometrial cancer.

Acknowledgments

This work was supported by the Natural Science Foundation of China (Grant no. 20875065; 21275101), Beijing Natural Science Foundation (Grant no. 2102010), and Beijing Municipal Knowledge Innovation Team Project (Grant no. PHR20100718).

References

[1] 〈http://globocan.iarc.fr〉.
[2] A.N. Fader, L.N. Arriba, H.E. Frasure, V.E. von Gruenigen, Gynecol. Oncol. 114 (2009) 121–127.

[3] Y. Xiang, K. Xu, Z. Zhang, Y. Dai, P.d.B. Harrington, J. Biomed. Opt. 15 (2010) 067002.
[4] Y. Norimatsu, H. Kouda, T.K. Kobayashi, K. Shimizu, K. Yanoh, C. Tsukayama, Y. Miyake, E. Ohno, Cytopathology 20 (2009) 395–402.
[5] A. Saadia, A. Mubarik, A. Zubair, S. Jamal, A. Zafar, J. Ayub Med. Coll. Abbottabad 23 (1) (2011) 129–131.
[6] A.K. Elfayomy, F.A. Habib, M.A. Alkabalawy, Arch. Gynecol. Obstet. 285 (2011) 839–843.
[7] J. Naftalin, N. Nunes, W. Hoo, R. Arora, D. Jurkovic, Ultrasound Obstet. Gynecol. 39 (2012) 106–109.
[8] E. Bignotti, M. Ragnoli, L. Zanotti, S. Calza, M. Falchetti, S. Lonardi, S. Bergamelli, E. Bandiera, R.A. Tassi, C. Romani, P. Todeschini, F.E. Odicino, F. Facchetti, S. Pecorelli, A. Ravaggi, Br. J. Cancer 104 (2011) 1418–1425.
[9] T. Tong, G. Yajia, W. Huaying, P. Weijun, Arch. Gynecol. Obstet. 285 (2011) 1113–1118.
[10] Z. Xiaobo, Z. Jiewen, M.J.W. Povey, M. Holmes, M. Hanpin, Anal. Chim. Acta 667 (2010) 14–32.
[11] T. Azzouz, R. Tauler, Talanta 74 (2008) 1201–1210.
[12] V. Bellon-Maurel, A. McBratney, Soil Biol. Biochem. 43 (2011) 1398–1410.
[13] R.M. Balabin, R.Z. Safieva, Anal. Chim. Acta 689 (2011) 190–197.
[14] J. Cai, Q. Chen, X. Wan, J. Zhao, Food Chem. 126 (2011) 1354–1360.
[15] V.R. Kondepati, M. Keese, R. Mueller, B.C. Manegold, J. Backhaus, Vib. Spectrosc. 44 (2007) 236–242.
[16] Q. Chen, J. Zhao, M. Liu, J. Cai, J. Liu, J. Pharma. Biomed. Anal. 46 (2008) 568–573.
[17] X. Zou, J. Zhao, H. Mao, J. Shi, X. Yin, Y. Li, Appl. Spectrosc. 64 (2010) 786–794.
[18] Y.P. Du, Y.Z. Liang, J.H. Jiang, R.J. Berry, Y. Ozaki, Anal. Chim. Acta 501 (2004) 183–191.
[19] J.H. Jiang, R.J. Berry, H.W. Siesler, Y. Ozaki, Anal. Chem. 74 (2002) 3555–3565.
[20] Q. Shen, W.M. Shi, W. Kong, B.X. Ye, Talanta 71 (2007) 1679–1683.
[21] H.L. Chen, B. Yang, J. Liu, D.Y. Liu, Expert Syst. Appl. 38 (2011) 9014–9022.
[22] H. Li, Y. Liang, Q. Xu, Chemom. Intell. Lab. Syst. 95 (2009) 188–198.
[23] S.W. Lin, K.C. Ying, S.C. Chen, Z.J. Lee, Expert Syst. Appl. 35 (2008) 1817–1824.
[24] J. García-Nieto, E. Alba, L. Jourdan, E. Talbi, Inf. Process. Lett. 109 (2009) 887–896.
[25] H. Xu, B. Qi, T. Sun, X. Fu, Y. Ying, J. Food Eng. 109 (2012) 142–147.
[26] M. Arakawa, Y. Yamashita, K. Funatsu, J. Chemom. 25 (2011) 10–19.
[27] S.W. Lin, Z.J. Lee, S.C. Chen, T.Y. Tseng, Appl. Soft Comput. 8 (2008) 1505–1512.
[28] F. Allegrini, A.C. Olivieri, Anal. Chim. Acta 699 (2011) 18–25.
[29] F. Melgani, Y. Bazi, IEEE Trans. Inf. Technol. Biomed. 12 (2008) 667–677.
[30] R. Gang, Z. Zhuping, Expert Syst. Appl. 38 (2011) 10420–10424.
[31] T. Cura, Expert Syst. Appl. 39 (2012) 1582–1588.
[32] J. Kennedy, R.C. Eberhart, IEEE Int. Conf. Neural Netw. 4 (1995) 1942–1948.
[33] F. Al-Obeidat, N. Belacel, J.A. Carretero, P. Mahanti, Appl. Soft Comput. 11 (2011) 4971–4980.
[34] A. Carlisle, G. Dozier, in: Proceedings of the Workshop Particle Swarm Optimization (2001) 1–6.
[35] J. Kennedy, R.C. Eberhart, IEEE Int. Conf. Syst. Man Cybern. 5 (1997) 4104–4108.
[36] V.N Vapnik, The Nature of Statistical Learning Theory, Springer-Verlag, New York, 1995.
[37] Z. Xu, C.E. Bunker, P.d.B. Harrington, Appl. Spectrosc. 64 (2010) 1251–1258.
[38] N. Qi, Z. Zhang, Y. Xiang, P.d.B. Harrington, Anal. Chim. Acta 724 (2012) 12–19.